Int. J. Electrochem. Sci., 10 **(2015)** 4004 - 4019

International Journal of
ELECTROCHEMICAL
SCIENCE
www.electrochemsci.org

5-Methyl-2,4-dihydropyrazol-3-one and 5-methyl-2-phenyl-2,4-didhydropyrazol-3-one as Copper Corrosion Inhibitors in Acidic Media

Andrés Díaz-Gómez[1,*], *Rosa Vera*[1], *Aurora Molinari*[1], *Alfonso Oliva*[1], *William Aperador*[2]

[1]Institute of Chemistry, Faculty of Sciences, Pontificia Universidad Católica de Valparaíso, Av. Universidad 330, Placilla, Valparaíso, Chile.
[2]Faculty of Engineering, Universidad Militar Nueva Granada, Carrera 1 101 - 80, Bogotá, Colombia.
[*]E-mail: andresdiaz.qind@gmail.com

Received: 13 January 2015 / *Accepted:* 28 February 2015 / *Published:* 23 March 2015

The present study analyses the copper corrosion behaviour of 5-methyl-2,4-dihydropyrazol-3-one (MHPO) and 5-methyl-2-phenyl-2,4-dihydropyrazol-3-one (MPPO) in 0.1 M sulphuric acid, using loss of mass, polarization curves (PC) and electrochemical impedance spectroscopy (EIS). The electrochemical results show that these organic compounds are mixed inhibitors that act preferentially on cathodic sites, inhibiting corrosion by blocking active sites on the metal surface. Changes in electrochemical parameters are related to the adsorption of the organic inhibitors on the metal surface, leading to the formation of a protective film which grows with the increase in exposure time in the medium. The adsorption of both compounds obeys Langmuir's adsorption isotherm and is physical in nature. Their inhibition efficiencies are favoured by high E_{HOMO} energy, and by a decrease in the E_{L-H} energy gap.

Keywords: Corrosion, copper, organic inhibitor, coating, acidic medium.

1. INTRODUCTION

Copper is widely used in various pipe systems for transporting water and for heat exchange. This is mainly due to its advantageous properties, such as: electrical and thermal conductivity, mechanical workability and significant resistance to corrosion [1-3]. However, incrustations and corrosion products adhering to the metal surface have a negative effect on heat exchange equipments, causing decreased efficiency, which in turn leads to the need for periodic cleaning of the oxidised metal using acidic solutions of H_2SO_4 or HCl. It is therefore necessary to use inhibiting compounds that, when added to the aggressive medium in small amounts, decrease the copper corrosion rate

through the formation of a coating over the surface of the metal, acting as a protective barrier that blocks active sites where corrosion processes mainly occur [4-5]. In general, organic heterocyclic compounds with active atoms in their structure, such as nitrogen, sulphur and oxygen [6-9], and which also possess conjugated polar functional groups [10], are considered efficient inhibitors of corrosion processes for copper and other materials [1-15].

The present study analyses the inhibition capacity of two organic heterocyclic compounds, 5-methyl-2,4-dihydropyrazol-3-one (MHPO) and 5-methyl-2-phenyl-2,4-dihydropyrazol-3-one (MPPO) of copper corrosion in 0.1 M H_2SO_4, using the techniques of mass loss, polarization curves and electrochemical impedance spectroscopy. Their inhibiting effects were corroborated theoretically with quantum chemical calculations DFT B3LYP/6-31G (d). The structures of the MHPO and MPPO are shown in Figure 1.

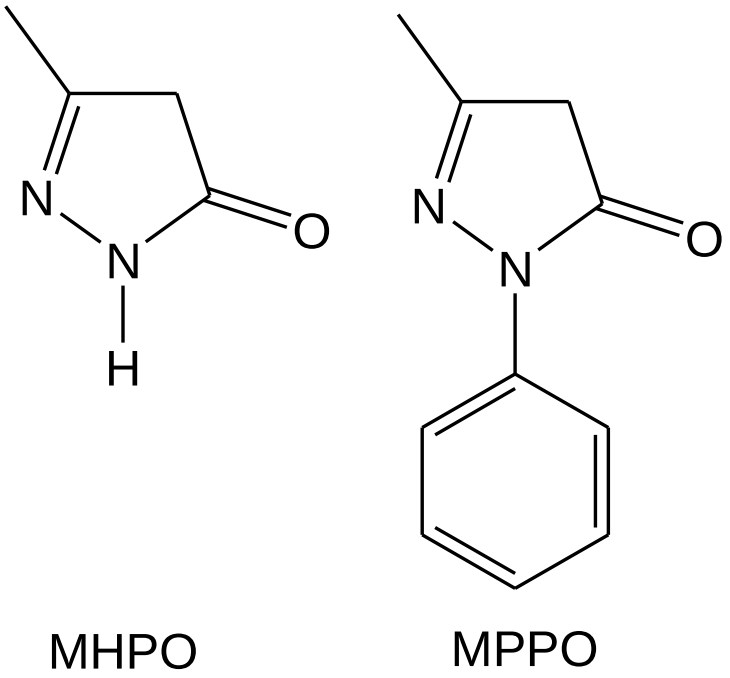

Figure 1. Structure of MHPO and MPPO.

2. EXPERIMENTAL PROCEDURE

2.1 Reagents and Materials

MHPO was synthesized from ethyl acetoacetate and hydrazine [16-17] while MPPO was a Merck commercial product. To obtain surfaces with low level of roughness, the copper metal samples of 99.37 % purity were polished with abrasive paper of 100 to 1200 increasing SiC grip and then with Al_2O_3 suspensions 1.0 and 0.05 μm on a spinning disc. The samples were degreased with acetone and air dried.

2.2 Mass Loss

Copper pieces measuring 5x5x0.3 cm were used in the experiments. They were submerged in a solution of 0.1 M H_2SO_4 in the absence and in the presence of the compounds MHPO and MPPO ($1x10^{-3}$ M). The testing was carried out in triplicate and with several different exposure times (5 hours and 7, 14 and 21 days) [18].

2.3 Polarization Curves

Polarization curves were obtained using a GSec 2.0 potentiostat-galvanostat in a conventional three-electrode cell. The working electrode was prepared as described in point 2.1 with an exposed area of 1 cm^2. The solution used was 0.1M H_2SO_4 in the presence and in the absence of the organic compounds. The potential of the working electrode was measured as a function of a saturated calomel reference electrode (SCE) connected to the solution via a Luggin capillary. A platinum wire (99.99 % Pt) was used as the auxiliary electrode. The Tafel polarization curves were obtained in an aerated solution at 25 °C and at a scan rate of 0.2 mV s^{-1}.

2.4 Electrochemical Impedance Spectroscopy (EIS)

A Gamry model PCI-4 potentiostat-galvanostat was used to evaluate EIS. The testing was carried out at a temperature of 25°C using the 0.1 M H_2SO_4 solution in the presence and in the absence of the inhibitors. The testing was also conducted as a function of time, over 5 hours and 7, 14 and 21 days. The apparatus used comprises a cell with a platinum counter-electrode (99.99 % Pt), and Ag/AgCl reference electrode, and copper pieces with an exposed area of 1 cm^2 as the working electrode. Nyquist plots were obtained from a scan in the frequency range of 0.001 Hz to 100 kHz, using a sinusoidal signal with an amplitude of 10 mV at open circuit potential (OCP).

2.5 Surface Characterization

The attack morphology of the copper corrosion in 0.1 M H_2SO_4 was observed under SEM using a Carl Zeiss Evo MA 10 coupled to an Oxford X-Act EDS analyser for elemental characterization.

2.6 Quantum Chemical Calculations

For the theoretical study, complete geometry optimisations of the MHPO and MPPO derivatives were performed using Density Functional Theory (DFT) with Beck's three-parameter exchange function and the Le–Yang–Par non-local correlation function (B3LYP) [19-2] with the 6-31G(d) basis set of atomic orbitals implemented in the Gaussian 09 software package.

3. RESULTS AND DISCUSSION

3.1 Mass Loss

By measuring mass loss, it was possible to analyse the copper dissolution in the 0.1 M H_2SO_4 medium in the absence and the presence of the organic compounds (MHPO and MPPO) as a function of exposure time. The corrosion rate (CR), degree of covered surface area (θ) and the inhibition efficiency percentage ($IE\%$) were calculated with the following equations [23]:

$$CR(mmpy) = 8.76\ X\ 10^3 \left(\frac{m_1 - m_2}{Spt}\right) \quad (1)$$

$$\theta = \frac{CR_0 - CR}{CR_0} \quad (2)$$

$$IE\% = \left(\frac{CR_0 - CR}{CR_0}\right) x\ 100 \quad (3)$$

where m_1 is the mass of the test probe before exposure in the aggressive medium, m_2 is the mass of the test probe after exposure, S is the total geometric area of the probe that as exposed, p is the copper density (8.94 g/cm^3), t is the exposure time, and CR_0 and CR are the corrosion rates in millimetres per year (mmpy) with and without inhibitor, respectively. The corrosion parameters, such as inhibition efficiency ($IE\%$) and corrosion rate (CR) in the absence and presence of the inhibitors (MHPO and MPPO) in 0.1 M H_2SO_4, are shown in Table 1.

Table 1. Mass loss for copper in 0.1 M H_2SO_4 in the presence and absence of inhibitor (MHPO and MPPO) at different exposure times.

Exposure time	Inhibitor ($1x10^{-3}$ M)	Weight loss (mg)	CR (mmpy)	Θ	$IE\%$
5 hours	Blank	9.02	0.35	-	-
	MHPO	5.65	0.22	0.37	37.14
	MPPO	4.75	0.18	0.49	48.57
7 Days	Blank	176,27	0.21	-	-
(168 hours)	MHPO	90,23	0.10	0.52	52.38
	MPPO	73.34	0.08	0.62	61.90
14 Days	Blank	324.67	0.18	-	-
(336 hours)	MHPO	129.73	0.07	0.61	61.11
	MPPO	115.92	0.06	0.67	66.66
21 Days	Blank	423.74	0.17	-	-
(504 hours)	MHPO	168.12	0.06	0.65	64.70
	MPPO	116.78	0.04	0.77	76.47

As can be seen in Table 1, both inhibitors, MHPO and MPPO, achieve inhibition of the copper corrosion process when added to the solution 0.1 M H_2SO_4, with MPPO giving higher inhibition

efficiency (76.47%) after 21 days of exposure. The corrosion rates decreased with increased exposure time in the acidic medium in the presence of the inhibitors. This may be due to the formation of a compact protective film composed of copper corrosion products and organic compounds adsorbed on the metal surface [10].

Figure 2 shows an SEM image of the copper samples after submersion in the 0.1 M H_2SO_4 solution for a period of 21 days at 303 K in the absence and presence of MPPO at a concentration of $1x10^{-3}$ M. The copper surface in the absence of MPPO (Fig. 2a) shows a rough corrosion product whose main elements when analysed by EDS are copper and oxygen. On the other hand, the copper submerged in the solution containing MPPO (Fig. 2b) shows corrosion product that is less rough in appearance, thus corroborating the protective effect of the organic compound. The EDS analysis of the surface gives copper, carbon, oxygen and nitrogen as the main elements, confirming the presence of a layer of MPPO adsorbed on the copper surface.

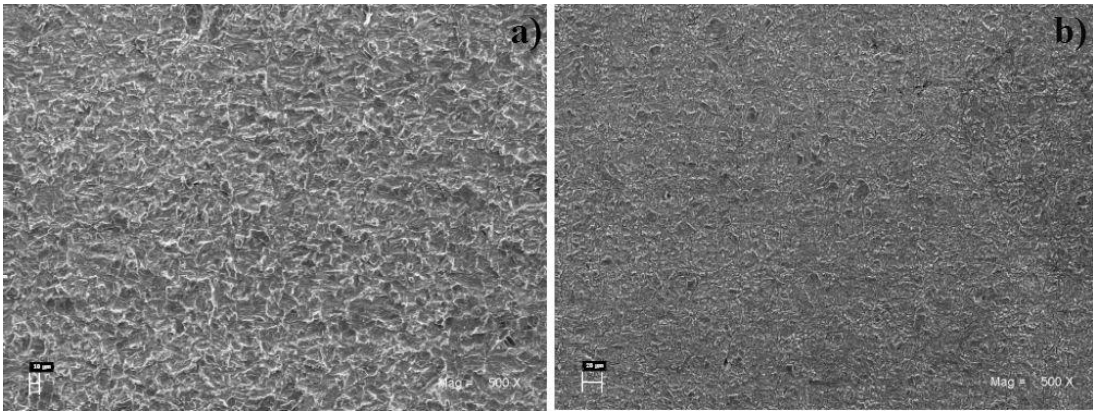

Figure 2. SEM images of the copper in 0.1 M H_2SO_4 after 21 days' exposure. a) absence b) presence of MPPO at $1x10^{-3}$ M.

The accepted mechanism for copper dissolution in acidic media in the absence of a complexing or inhibiting agent is described by the following two steps (Scheme 1) [24]:

Fast

$$Cu_{(s)} \longleftrightarrow Cu^{+}_{(ads)} + e^{-}$$

Slow

$$Cu^{+}_{(ads)} \longleftrightarrow Cu^{2+}_{(sol)} + e^{-}$$

Scheme 1. Anodic copper dissolution mechanism in acidic media.

The cathodic reduction of oxygen can be expressed by a transfer of 4e-, or two consecutive steps involving a reduction to hydrogen peroxide followed by an additional reduction (Scheme 2) [25].

Global reaction

$$O_{2(g)} + 4H^+ + 4e^- \longleftrightarrow 2H_2O_{(l)}$$

Two step

$$O_{2(g)} + 2H^+ + 2e^- \longleftrightarrow H_2O_{2(aq)}$$

$$H_2O_{2(aq)} + 2H^+ + 2e^- \longleftrightarrow 2H_2O_{(l)}$$

Scheme 2. Oxygen cathodic reduction mechanism.

When an organic molecule [$Org_{(sol)}$] is adsorbed onto the metal/solution interface, it replaces one or more adsorbed water molecules [$H_2O_{(ads)}$] on the metal surface (Scheme 3), where "n" represents the number of molecules of water replaced by an adsorbed organic molecule [26].

$$Org_{(sol)} + nH_2O_{(ads)} \longleftrightarrow Org_{(ads)} + nH_2O_{(sol)}$$

Scheme 3. Adsorption mechanism of an organic molecule on the metal/solution interface.

3.2 Polarization Curves

The copper polarization curves in 0.1 M H_2SO_4 in the absence and presence of inhibitor (MHPO and MPPO) are shown in Figure 3. In the presence of the inhibitors, a decrease in corrosion potential and a slight variation in current density towards lower values can be seen.

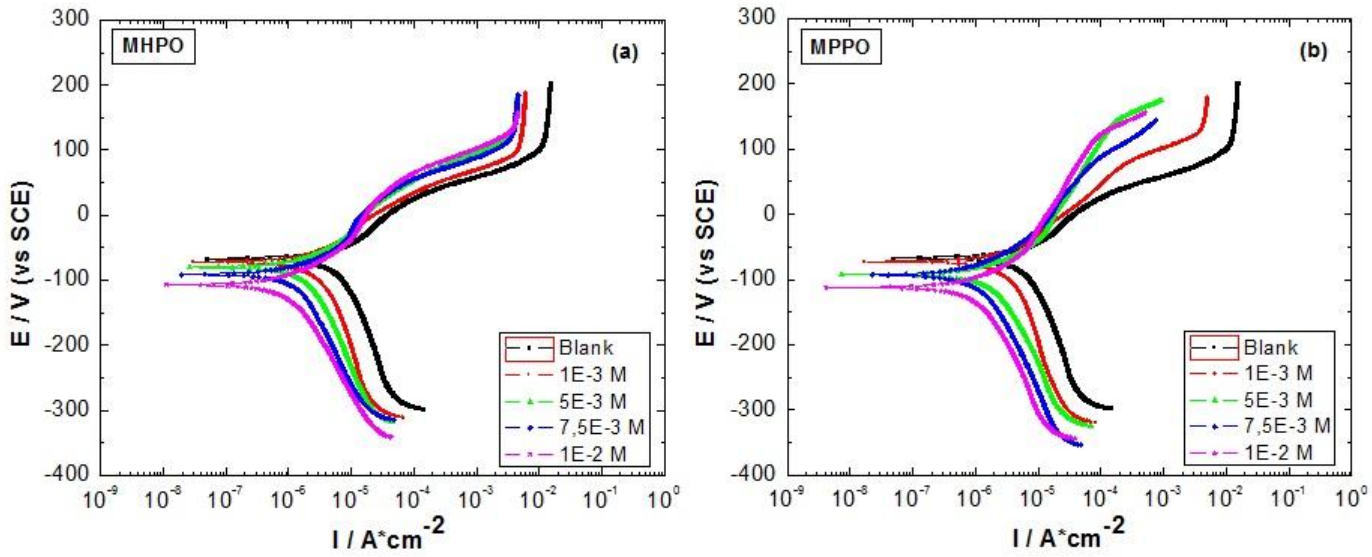

Figure 3. Copper polarization curves in 0.1 M H_2SO_4 in the absence and presence of inhibitor at 25° C. (a) MHPO and (b) MPPO

The anodic and cathodic current-potential curves are extrapolated to an intersection point, where the corrosion current density (i_{corr}) and the corrosion potential (E_{corr}) are obtained [27]. The electrochemical parameters, i_{corr} and E_{corr}, anodic and cathodic slopes (β_c, β_a) obtained from the polarization curves (Fig. 3) are shown in Table 2.

Table 2. Parameters of copper polarization curves in 0.1 M H_2SO_4 in the absence and presence of inhibitor at 25° C at different MHPO and MPPO concentrations.

Concentration ($1x10^{-3}$ M)	i_{corr} ($\mu A/cm^2$)	E_{corr} (mV/SCE)	β_c (mV/dec)	β_a (mV/dec)	*IE%*
Blank	5.38	-68	106.6	55.6	-
MHPO 1	1.93	-71	88.6	54.8	64.2
5	1.46	-80	91.8	48.4	72.8
7.5	1.16	-91	96.1	48.6	78.5
10	0.77	-106	79.0	46.6	85.6
MPPO 1	1.53	-73	90.4	56.6	71.6
5	1.21	-92	73.9	51.8	77.5
7.5	1.02	-94	80.0	52.1	81.1
10	0.56	-112	87.9	50.0	89.6

Table 2 shows that the increase in inhibitor concentration leads to a decrease in corrosion current (i_{corr}) and a subsequent increase in the inhibition efficiency percentage (*IE%*). The inhibitor that best blocks the active sites where corrosion processes occur on the copper in 0.1 M H_2SO_4 is the MPPO, with an *IE%* of 89.6% at a concentration of $1x10^{-2}$ M. The table also shows the shift in E_{corr} towards more negative values in the presence of MHPO and MPPO which indicates that the inhibitors have more influence on the cathodic reduction of oxygen than on the copper oxidation reaction. Moreover, a decrease both cathodic (β_c) and anodic (β_a) Tafel slopes suggest that the organic compounds MHPO and MPPO to be classified as mixed inhibitors that act preferentially on cathodic sites [28-29].

3.3 Adsorption Isotherm

Assuming a direct relationship between inhibition efficiency (*IE%*) and surface coverage [$IE\% = \theta$ x 100] for different inhibitor concentrations, the data from the polarization curve measurements can be adapted to calculate the adsorption parameters of the MHPO and MPPO on copper in 0.1 M H_2SO_4 at 25°C. In order to obtain the best fit, several adsorption isotherms were tested, such as Langmuir, Temkin and Frumkin [3], [30]. The results show that the Langmuir isotherm best describes the adsorption of the molecules in question on the copper surface. The Langmuir isotherm is given in equation 4 [31].

$$\frac{C}{\theta} = C + \left(\frac{1}{K}\right) \qquad (4)$$

where C is the concentration of the inhibitor, θ is fraction of covered surface area and K is the adsorption equilibrium constant related to the free adsorption energy (ΔG°_{ads}) (equation 5).

$$K = \left(\frac{1}{C_{solvent}}\right) \exp\left(\frac{-\Delta G^{\circ}_{ads}}{RT}\right) \quad (5)$$

where $C_{solvent}$ represents the molar concentration of the solvent, which in the case of water is 55.5 mol l^{-1}, R is the universal gas constant and T is the system temperature. The graph of C/θ vs. C (Eq. 4) gives a linear relationship with a slope close to 1 and a coefficient of correlation (R^2) of 0.999. In this situation, the value of the equilibrium constant (K) can be calculated as the inverse of the intercept (Fig. 4) [32]. The free adsorption energy (ΔG°_{ads}) is found from the equilibrium constant (K) using eq. 5. The values calculated for the adsorption constant and the free adsorption energy (ΔG°_{ads}) are shown in Table 3.

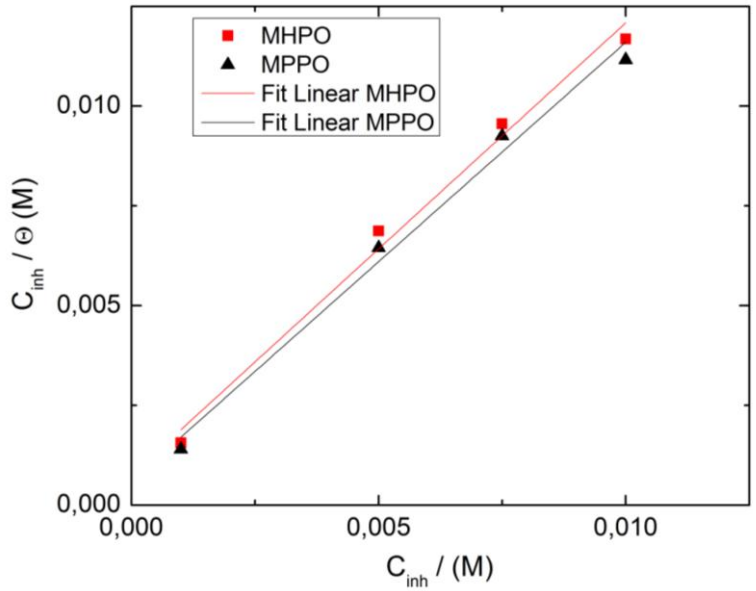

Figure 4. Langmuir adsorption isotherm of organic compounds MHPO and MPPO on the copper surface in 0.1 M H_2SO_4 at 25° C.

Table 3. Langmuir adsorption isotherm parameters for MHPO and MPPO on the copper surface in 0.1 M H_2SO_4 at 25° C.

Inhibitor	K 1x10^3 (L/mol)	ΔG°_{ads} (KJ/mol)
MHPO	1.33	-27.8
MPPO	1.67	-28.3

The negative values of (ΔG°_{ads}) indicate spontaneity in the adsorption process and stability of the MHPO and MPPO when adsorbed onto the copper surface. It is known that the values of (ΔG°_{ads})

close to -20 KJ/mol or higher are consistent with electrostatic interactions between the charges of the organic compound and the charges of the metal surface (physisorption). However, values of (ΔG°_{ads}) close to -40 KJ/mol or less are related to charge exchange or transfer from the organic molecule to the metal surface as a type of coordination bond (chemisorption) [3-34]. For MHPO and MPPO, the values calculated for (ΔG°_{ads}) are -27.8 KJ/mol and -28.3 KJ/mol, respectively, suggesting that the adsorption mechanism for both organic compounds is closer to physisorption.

3.4 Electrochemical Impedance Spectroscopy (EIS)

Figure 5 shows the Nyquist plots obtained for the MHPO and MPPO on a copper surface in 0.1 M H_2SO_4 at different exposure times (5 hours and 7, 14 and 21 days). The Nyquist semicircles are generally associated with a charge transfer on the electrode/electrolyte interface, an electrical double layer, and their diameters are related to the resistance with which the interface opposes the charge transfer [8].

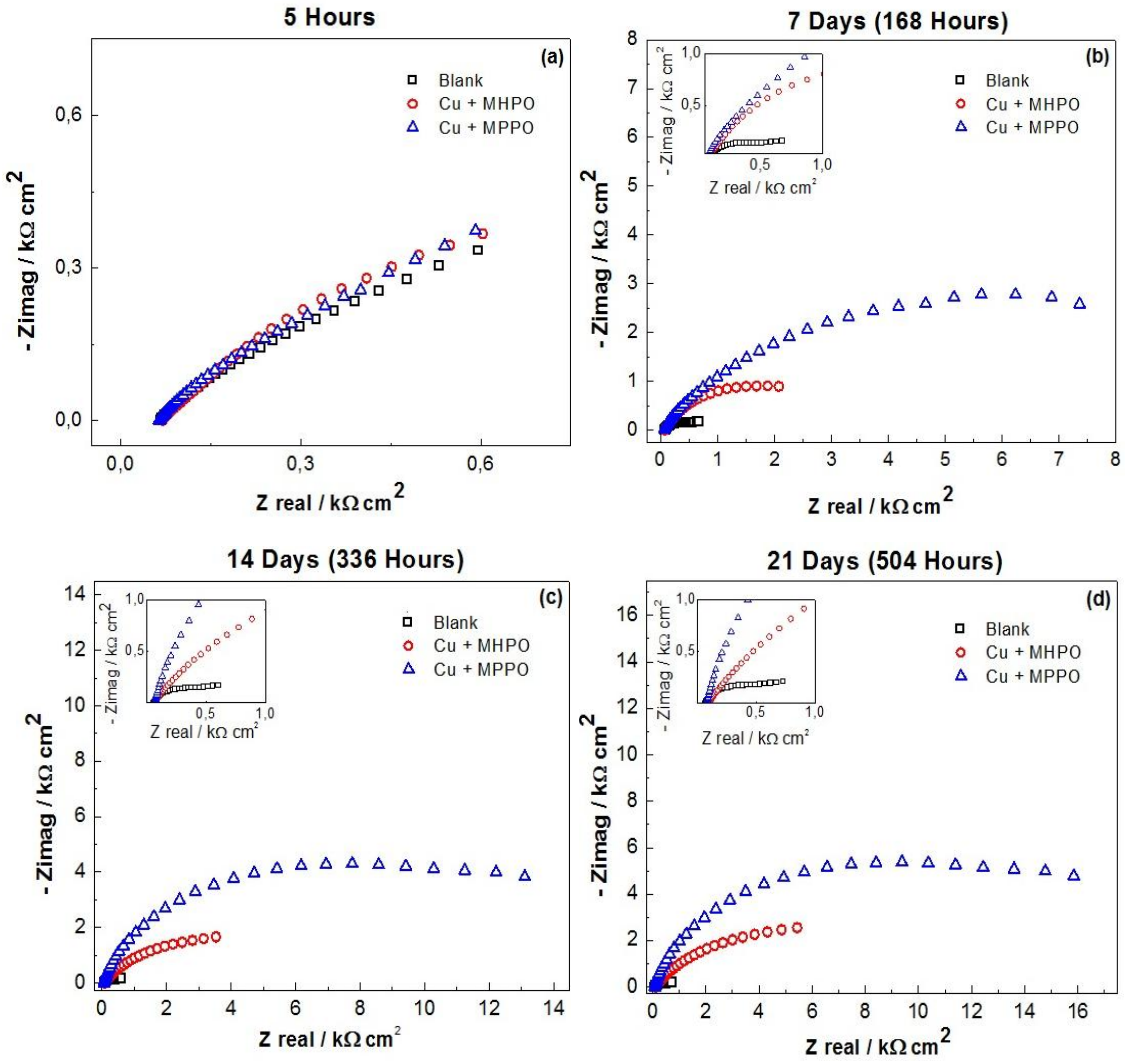

Figure 5. Nyquist plots of MHPO and MPPO ($1x10^{-3}$ M) on the copper surface in 0.1 M H_2SO_4 at different exposure times. (a) 5 hours; (b) 7 days; (c) 14 days; and (d) 21 days.

The Nyquist plots in Figure 5 were fit with the equivalent circuit represented in Figure 6, where R_s represents the resistance to the solution, R_{ct} is the polarization resistance of the charge transfer through the film and R_f is the polarization resistance of the film/electrolyte interface. CPE_{ct} is a constant phase element used to modify the capacitance of the electrical double layer to obtain more accurate results. The parameters obtained from fitting the EIS curves for the copper with and without inhibitor ($1x10^{-3}$ M) at different exposure times are shown in Table 4. The inhibition efficiency (*IE%*) was calculated in accordance with equation 6 [35].

$$IE\% = \frac{R_p - R_p^{\circ}}{R_p} x100 \qquad (6)$$

where R_p *y* R_p° are the total polarization resistances of the copper in 0.1 M H_2SO_4 with and without inhibitor, respectively, and $R_p = R_f + R_{ct}$. The calculated values $IE\%$ are shown in Table 4, and it can be seen that these increase with exposure time.

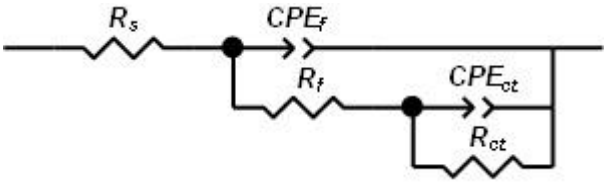

Figure 6. Equivalent circuit used for MHPO and MPPO on the copper surface in 0.1 M H_2SO_4.

Table 4. Parameters obtained from fitting the EIS curves for the copper with and without inhibitor ($1x10^{-3}$ M) in 0.1 M H_2SO_4 at different exposure times.

Time days	R_s (Ω cm^2)	CPE_f ($\mu F\ cm^{-2}\ s^{-(1-\alpha 1)}$)	α_1	R_f (kΩ cm^2)	CPE_{ct} ($\mu F\ cm^{-2}\ s^{-(1-\alpha 2)}$)	α_2	R_{ct} (kΩ cm^2)	R_p (kΩ cm^2)	*IE%*
Blank									
5 hours	43.5	1.46	0.87	0.58	4.23	0.84	1.61	2.19	-
7	38.1	1.44	0.81	0.56	4.12	0.79	1.43	1.99	-
14	38.6	1.04	0.70	0.31	3.43	0.78	1.35	1.66	-
21	43.2	1.12	0.71	0.32	3.65	0.73	1.24	1.56	-
MHPO									
5 hours	65.1	2.45	0.82	0.87	6.22	0.82	2.73	3.60	39.2
7	72.3	5.38	0.79	1.02	10.22	0.72	3.67	4.69	57.6
14	68.8	5.39	0.91	1.51	29.54	0.69	6.51	8.02	79.3
21	69.3	6.98	0.84	4.03	46.54	0.92	9.85	13.88	88.8
MPPO									
5hours	66.1	5.12	0.72	1.12	12.21	0.71	5.26	6.38	65.7
7	68.6	7.62	0.84	3.75	19.65	0.69	8.43	12.18	83.7
14	65.3	24.12	0.79	5.33	57.77	0.85	19.01	24.34	93.2
21	63.8	23.21	0.81	6.80	86.54	0.88	22.62	29.42	94.7

The values of R_p for the copper increase with exposure time in the 0.1 M H_2SO_4 in the presence of MHPO and MPPO, giving a higher value for R_p with the latter compound, and therefore a higher *IE%* (94.7%) at 21 days of exposure. The increase with time (Fig. 7) may be due to organic molecules that are adsorbed onto the copper surface forming a film that acts as a physical barrier that opposes resistance (R_f) to the transfer of electrons. This barrier also grows in time. It can also be seen that in the absence of inhibitors the copper is able to form a natural protective film which also shows resistance to electron transfer (R_f), and which significantly increases in the presence of the organic compounds in question.

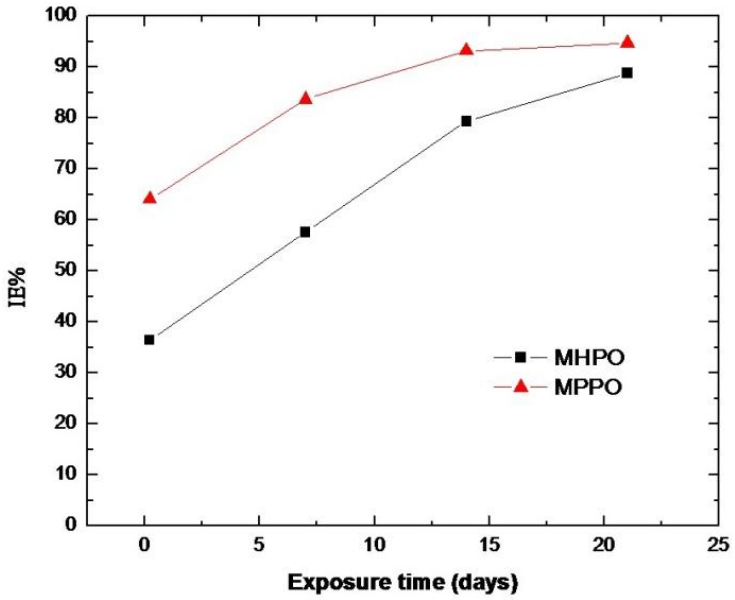

Figure 7. Inhibition efficiency with increased exposure time for MHPO and MPPO.

3.5 Quantum Chemical Calculations

Quantum chemical calculations were used to correlate the experimental data. The quantum MHPO and MPPO parameters were obtained using functional density theory (DFT) B3LYP/6-31G (d). The structures optimised by minimum energy for the organic compounds are shown in Figure 8. The reaction capacity of the inhibitors is strongly correlated with their frontier molecular orbitals (FMOs), considering the highest occupied molecular orbital (*HOMO*) and the lowest unoccupied molecular orbital (*LUMO*), as well as other parameters. According to this theory, chemical reactivity is a function of the interactions of the *HOMO* and *LUMO* levels of the reactive species. E_{HOMO} is a quantum chemical parameter associated with the capacity of the organic molecule to donate electrons. A high E_{HOMO} value indicates the tendency to donate electrons to an appropriate receptor system with low energy in the first empty molecular orbital. It also indicates the ability of the molecule to accept electrons. Therefore, the adsorption capacity of the organic molecule on the metal surface is favoured by an increase in E_{HOMO} and a decrease in E_{LUMO}. As a result, the value of $\Delta E_{L\text{-}H}$ gives a measurement of stability for the organic molecule when forming a complex on the metal surface. In this case, the

MPPO has a lower value (4.860 eV) than that of the MHPO (5.767 eV), and therefore MPPO has more stability and a higher probability of forming a surface complex. The calculations of all the quantum chemical parameters are shown in Table 5.

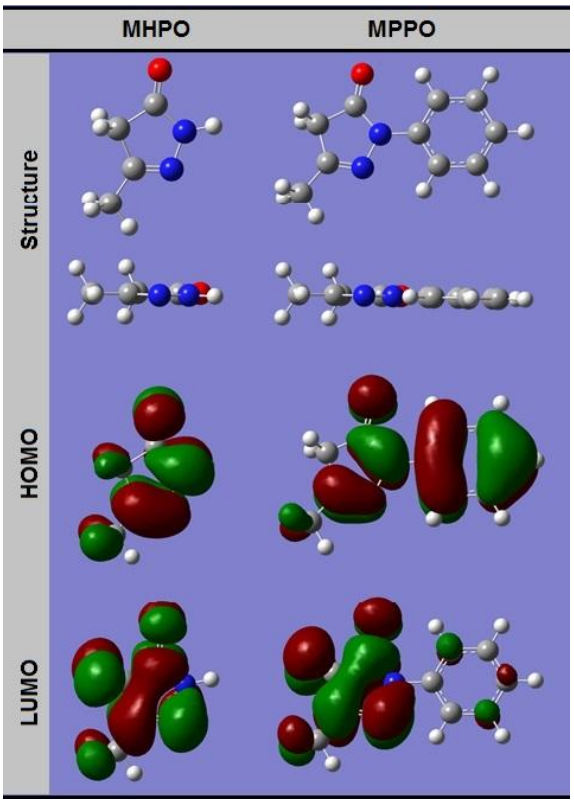

Figure 8. Optimised structures and molecular orbitals of MHPO and MPPO.

Table 5. Quantum parameters for MHPO and MPPO with B3LYP/6-31G (d).

Inhibitor	E_{HOMO} (eV)	E_{LUMO} (eV)	ΔE_{L-H} (eV)	μ (Debye)	I (eV)	A (eV)	χ (eV)	η (eV)	ΔN
MHPO	-6.427	-0.660	5.767	2.801	6.427	0.660	3.544	2.884	0.192
MPPO	-5.731	-0.871	4.860	3.308	5.731	0.871	3.301	2.430	0.278

Another important parameter is the dipole moment (μ) of the molecule, which is associated with an increase in inhibition and is also related to the dipole-dipole interaction of the organic molecule and the metal surface [36]. As shown in Table 5, the MPPO presents a higher dipole moment than that of the MHPO, 3.308 D and 2.801 D respectively, thus verifying that the MPPO has greater interaction with the metal surface, giving it a better inhibitory property than that of the MHPO. The fraction of transferred electrons (ΔN) from the organic molecule to the copper surface was calculated using equation 7 [37-38].

$$\Delta N = \frac{\chi_{Cu} - \chi_{Inh}}{2(\eta_{Cu} + \eta_{Inh})} \quad (7)$$

where χ_{Cu} y χ_{Inh} are the absolute electronegativity of the copper and the inhibitor, respectively; and η_{Cu} y η_{Inh} are the absolute hardness of the copper and the inhibitor, respectively.

The ionization potential (I) and electron affinity (A) are related to E_{HOMO} and E_{LUMO} as shown below, in accordance with Hartree-Fock theory:

$$I = -E_{\text{HOMO}} \quad (8)$$
$$A = -E_{\text{LUMO}}$$

These parameters are related to absolute electronegativity and absolute hardness via equations 9.

$$\chi = \frac{I + A}{2} \quad (9)$$
$$\eta = \frac{I - A}{2}$$

As there are two systems with different electronegativities, a metal surface and an organic molecule, the electron transfer mechanism that will take place is an electron flow from the species with lower electronegativity to the species with higher electronegativity, until the chemical potentials are the same. In order to calculate the fraction of electrons transferred during the adsorption process between the organic molecules and the metal surface, a theoretical electronegativity value for copper will be used, χ_{Cu}= 4.65 eV [38-39], also assuming a global hardness for the copper, η_{Cu}= 0; $I = A$. In Table 5 it can be seen that the molecule with lower hardness is MPPO (2.430 eV), and therefore, it will have better interaction with the metal surface of the copper, giving a larger fraction of transferred electrons (0.278 e) than that of the MHPO. This verifies the experimental values (mass loss, polarisation curves and EIS) of *IE%*, in which the MPPO shows better performance for copper corrosion inhibition in the acidic medium.

The Mulliken atomic charge distributions for the MHPO and MPPO are presented in Figure 9 and Table 6. In the literature it is reported that the most negative atomic charge of the adsorbed centre will more easily donate its electrons to a vacant orbital in the metal [40-41].

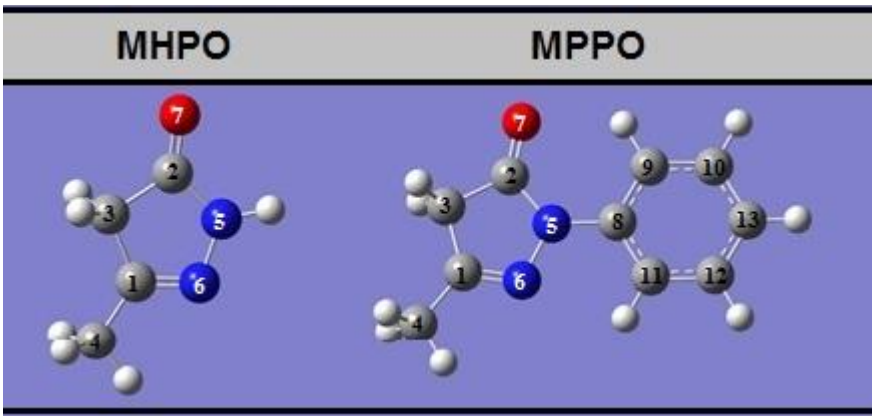

Figure 9. Mulliken charge distribution of MHPO and MPPO, using DFT B3LYP/6-31G (d).

Table 6. Mulliken atomic charges present in MHPO and MPPO.

N°	Atom	Charge	
		MHPO	MPPO
1	C	0.342	0.359
2	C	0.616	0.618
3	C	-0.468	-0.474
4	C	-0.517	-0.518
5	N	-0.468	-0.454
6	N	-0.272	-0.276
7	O	-0.495	-0.494
8	C		0.321
9	C		-0.174
10	C		-0.146
11	C		-0.122
12	C		-0.141
13	C		-0.163

The results shown in Table 6 corroborate that in the MHPO molecule the charge density is distributed along the pyrazole ring, mainly on the nitrogen and oxygen atoms, while in the MPPO, as well as the distribution on the pyrazole ring, the charge density is also distributed on the phenyl ring, thus favouring more interaction on the metal surface, probably in a planar structural formation, achieving better coverage of the surface of the metal.

4. CONCLUSIONS

The principal conclusions drawn from this study are the following:

- The organic compounds MHPO and MPPO show corrosion inhibition activity on the copper surface in 0.1 M H_2SO_4; both act as mixed inhibitors with a preference for inhibiting cathodic sites. For both inhibitors, an increment in concentration increases the *IE%*, which also occurs with increased exposure time.
- The organic compounds MHPO and MPPO show physical adsorption on the copper surface in accordance with the Langmuir isotherm, occurring as a spontaneous process in both cases.
- The experimental results obtained from the different techniques applied in the study are in agreement with the theoretical data, verifying that the MPPO compound presents better behaviour for copper corrosion inhibition in 0.1 M H_2SO_4, with a lower ΔE_{L-H} , a higher dipole moment, and a higher fraction of transferred electrons on the metal surface, as well as giving decreased roughness on

the copper surface and showing the presence of nitrogen pertaining to the organic compound as confirmed by EDX analysis.

ACKNOWLEDGEMENTS
The authors acknowledge the support of the Government of Chile through doctoral scholarship funds (Conicyt 211052) and the Department of Research at the Pontificia Universidad Católica de Valparaíso.

References

1. R. Vera, F. Bastidas, M. Villarroel, A. Oliva, A. Molinari, D. Ramírez, and R. del Río, *Corros. Sci.*, 50 (2008) 729.
2. X. Liao, F. Cao, L. Zheng, W. Liu, A. Chen, J. Zhang, and C. Cao, *Corros. Sci.*, 53 (2011) 3289.
3. H. Tian, W. Li, K. Cao, and B. Hou, *Corros. Sci.*, 73 (2013) 281.
4. M. A. Amin and K. F. Khaled, *Corros. Sci.*, 52 (2010) 1194.
5. R. Vera, A. Oliva, and A. Molinari, *Heterocycles Lett.*, 1 (2011) 158.
6. K. F. Khaled, *Corros. Sci.*, 52 (2010) 3225.
7. L. Feng, H. Yang, and F. Wang, *Electrochim. Acta*, 58 (2011) 427.
8. H. Ma, S. Chen, L. Niu, S. Zhao, S. Li, and D. Li, *J. Appl. Electrochem.*, 32 (2002) 65.
9. D. Zhang, L. Gao, and G. Zhou, *Appl. Surf. Sci.*, 225 (2004) 287.
10. H. Otmačić and E. Stupnišek-Lisac, *Electrochim. Acta*, 48 (2003) 985.
11. S. Ramesh and S. Rajeswari, *Corros. Sci.*, 47 (2005) 151.
12. M. N. El-Haddad, *Int. J. Biol. Macromol.*, 55 (2013) 142.
13. N. a. Al-Mobarak, K. F. Khaled, M. N. H. Hamed, K. M. Abdel-Azim, and N. S. Abdelshafi, *Arab. J. Chem.*, 3 (2010) 233.
14. S. S. Abdel-Rehim, K. F. Khaled, and N. a. Al-Mobarak, *Arab. J. Chem.*, 4 (2011) 333.
15. M. M. Antonijevic and M. B. Petrovic, *Int. J. Electrochem. Sci.*, 3 (2008) 1.
16. J. Buchi and R. Ursprung, *Helv. Chim. Acta*, 32 (1949) 984.
17. P. Villalobos, C. Castillo, and A. Oliva, *Bol. Soc. Chil. Quim.*, 36 (1991) 117.
18. ASTM, "Standard Practice for Laboratory Immersion Corrosion Testing of Metals. G 31," 2004.
19. A. Becke, *J. Chem. Phys.*, 96 (1992) 2155.
20. A. Becke, *J. Chem. Phys.*, 97 (1992) 9173.
21. A. Becke, *J. Chem. Phys.*, 98 (1993) 1372.
22. C. Lee, W. Yang, and R.G. Parr, *Phys. Rev. B.*, 37 (1988) 785.
23. M. Scendo, *Corros. Sci.*, 50 (2008) 2070.
24. E. Mattsson and J. O. Bockris, *Trans. Faraday Soc.*, 55 (1959) 1586.
25. P.Jinturkar, Y.C. Guan, K.N. Han, *Corrosion*, 54 (1984) 106.
26. J. O. Bockris and D. a. J. Swinkels, *J. Electrochem. Soc.*, 111 (1964) 736.
27. E.-S. M. Sherif, R. M. Erasmus, and J. D. Comins, *J. Colloid Interface Sci.*, 309 (2007) 470.
28. G. Quartarone, M. Battilana, L. Bonaldo, and T. Tortato, *Corros. Sci.*, 50 (2008) 3467.
29. H. Vaidyanathan and N. Hackerman, *Corros. Sci.*, 11 (1971) 737.
30. W. Li, Q. He, C. Pei, and B. Hou, *Electrochim. Acta*, 52 (2007) 6386.
31. I. Ahamad, R. Prasad, and M. a. Quraishi, *Corros. Sci.*, 52 (2010) 3033.
32. G. Quartarone, L. Bonaldo, and C. Tortato, *Appl. Surf. Sci.*, 252 (2006) 8251.
33. R. Solmaz, *Prog. Org. Coatings*, 70 (2011) 122.
34. A. Gazi and M. Madz, 47 (2002) 2.
35. E. M. Sherif and S.-M. Park, *Electrochim. Acta*, 51 (2006) 6556.
36. B. D. Mert and B. Yazıcı, *Mater. Chem. Phys.*, 125 (2011) 370.

37. K. F. Khaled, *Mater. Chem. Phys.*, 112 (2008) 104.
38. R. G. Pearson, *Inorg. Chem.*, 27 (1988) 734.
39. H. B. Michaelson, *J. Appl. Phys.*, 48 (1977) 4729.
40. I. B. Obot and N. O. Obi-Egbedi, *Mater. Chem. Phys.*, 122 (2010) 325.
41. I. B. Obot and N. O. Obi-Egbedi, *Colloids Surface A.*, 330 (2008) 207.